IDENTIFICATION OF THE ATTITUDE DYNAMICS FOR A VARIABLE-PITCH QUADROTOR UAV

Fabio Riccardi
Dipartimento di Scienze
e Tecnologie Aerospaziali
Politecnico di Milano
Via la Masa 34
20156 Milano, Italy
fabio.riccardi@polimi.it

Pietro Panizza
Dipartimento di Elettronica,
Informazione e Bioingegneria
Politecnico di Milano
Piazza Leonardo da Vinci 32
20133 Milano, Italy
pietro.panizza@polimi.it

Marco Lovera
Dipartimento di Elettronica,
Informazione e Bioingegneria
Politecnico di Milano
Piazza Leonardo da Vinci 32
20133 Milano, Italy
marco.lovera@polimi.it

Abstract: System identification is an established approach for the derivation of control-oriented dynamic models in the rotorcraft field (see for example the survey paper [9], the recent books [19] [10] and the references therein). While the application to full scale rotorcraft is by now fairly mature, less experience has been gathered on small-scale vehicles, such as, *e.g.*, quadrotor UAVs. In this paper the problem of characterizing the attitude dynamics of a variable-pitch quadrotor from data is considered and the results obtained in an experimental identification campaign are presented and discussed. More precisely, in this study both on-line and off-line methods have been considered and the performance of black-box versus grey-box models has been compared.

NOMENCLATURE

A	rotor disk area
A_b	rotor blade area
c	damping of the IMU vibration damping system
C_{l_α}	blade airfoil lift curve slope
$\frac{\partial \frac{C_T}{\sigma}}{\partial \theta_R}$	rotor thrust coefficient over solidity curve slope respect to collective blade pitch angle
C_T	rotor thrust coefficient
d	quadrotor arm length
I	quadrotor inertia matrix
J	pitch axis inertia moment of IMU vibration damping system
k	spring rate of the IMU vibration damping system
Q	measurement noise variance
R	rotor radius
Γ	observability matrix
θ	quadrotor pitch
Θ	grey box model parameter vector
σ	rotor solidity
τ	closed-loop overall time delay
ϕ	quadrotor roll angle
ψ	quadrotor yaw angle
$\bar{\Omega}$	constant rotor angular velocity

1. INTRODUCTION AND MOTIVATION

Quadrotors have become increasingly popular in recent years as platforms for both research and commercial unmanned aerial vehicle (UAV) applications. In order to fully exploit the potential performance of such platforms, however, wide bandwidth attitude controllers must be designed. This, in turn, calls for accurate dynamic models of the vehicle's response to which advanced controller synthesis approaches can be applied. As discussed in, *e.g.*, [16] and the references therein, mathematical models for quadrotor dynamics are easy to establish as far the kinematics and dynamics of linear and angular motion are concerned. In fact a significant portion of the literature dealing with quadrotor control is based on such models. Unfortunately, characterizing aerodynamic effects and additional dynamics such as, *e.g.*, due to actuators and sensors, is far from trivial, and has led to the development of many approaches to the experimental characterization of the dynamic response of the quadro-

Figure 1: Aermatica Anteos on laboratory test-bed.

tor. More precisely, two classes of methods to deal with this problem can be envisaged. The first class of methods is based on black-box identification and aims at modeling the dynamics of the system directly (and solely) from measured input-output data (see for example [14]). The second class of methods is based on the calibration of the parameters of detailed physical models, see for example [12]. In the present framework, key requirements for the identification method and the model class are the degree of automation of the identification procedure and the compatibility of the model class with existing control synthesis tools. Meeting such requirements would enable a fast and reliable deployment of the vehicle's control system.

In view of the above discussion, this paper deals with the problem of characterizing the attitude dynamics of a variable-pitch quadrotor directly from data and presents the results obtained in an experimental identification campaign based on the Aermatica Anteos quadrotor UAV, a platform having a MTOW of about 5 kg and an arm length of $d = 0.415$ m with variable collective pitch - fixed rotor RPM architecture. More precisely, a number of different model identification methods have been considered in this study, with the aim of covering: on-line and off-line estimation, input-output and state space models, black-box and grey-box modeling approaches.

This paper is organized as follows: Section 2 presents the approach to model identification of the pitch dynamics as well as the corresponding experiments. In Section 3 the black-box model identification methods are illustrated. Subsequently, the grey-box methods are described in Section 4. Finally, Section 5 presents the results of the identification process; these results are then validated in the same section.

2. IDENTIFICATION EXPERIMENTS

The pitch attitude identification experiments discussed in this paper have been carried out in laboratory conditions, with the quadrotor placed on a test-bed that constrains all translational and rotational DoFs except for pitch rotation, as shown in Figure 1. Similar experiments have been carried out in flight to ensure that the indoor setup is representative of the actual attitude dynamics in flight for near hovering conditions.

Identification campaign	PRBS signal switching interval range [s]
1	$[0.05, 0.1]$
2	$[0.1, 0.2]$
3	$[0.2, 0.4]$
4	$[0.4, 0.8]$

Table 1: PRBS min/max switching intervals for the four identification campaigns.

The control variable of the real system is the difference between collective blade pitch on opposite rotors. Even in controlled laboratory conditions, the design of excitation sequences for the attitude dynamics of the quadrotor is a critical issue because of the inherent (fast) instability. In the present study a Pseudo Random Binary Sequence (PRBS, see [15]) was selected and applied in quasi open-loop conditions: while the nominal attitude and position controllers were disabled, a supervision task enforcing attitude limits during the experiment was left active. The parameters of the PRBS sequence (signal amplitude and min/max switching interval) were tuned to obtain an excitation spectrum consistent with the expected dominant attitude dynamics, between 3 rad/s and 6 rad/s.

Several PRBS sequences were tested, in order to obtain a spectrum with the main harmonic in the desired frequency range and a reduced second harmonic amplitude. More precisely, four different identification campaigns were conducted where the switching interval was varied. The PRBS min/max switching intervals in the different campaigns are reported in Table 1. In turn, each identification campaign is composed of three different identification tests that contain PRBS signals with different amplitudes: in the first one the signal switches between -0.012 rad and 0.012 rad, in the second one between -0.015 rad and 0.015 rad and in the last one the minimum and the maximum values of the signal are -0.019 rad and 0.019 rad respectively. As illustrated in Figure 2, the input signal of each identification experiment consists of three different PRBS excitation sequences (I, II, III in Figure 2) with the same switching interval and the same amplitude while in the last section of each identification test (IV in Figure 2), the nominal attitude controller was reactivated and a desired angular reference was manually imposed. This latter portion of each dataset is not tied to the parameters of the PRBS in the identi-

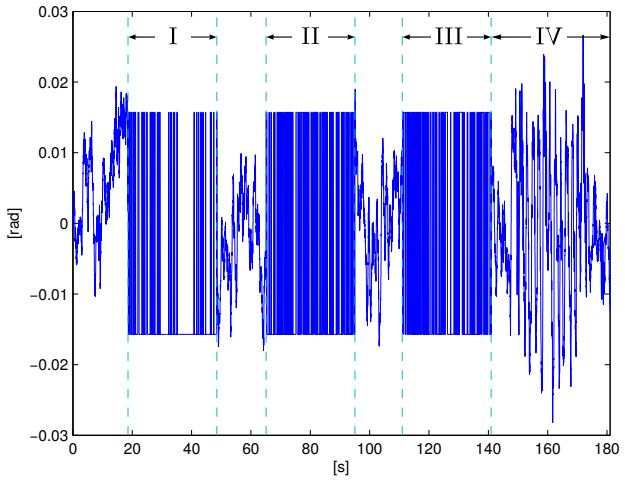

Figure 2: Input signal of an identification test, namely the difference between collective blade pitch on opposite rotors (I, II and III are three different PRBS excitation sequences; IV represents a typical flight condition where a desired angular reference is imposed).

fication experiment and is collected for validation purposes since it representative of a typical closed-loop flight condition. It is apparent from Figure 2 that the input sequence of each identification experiment contains portions of non-relevant information, *e.g.*, the periods between consecutive excitations. To deal with the identification of the real system, it is natural to extract from the original data only the segments that contain relevant information about the dynamics of the quadrotor. Thus, to obtain an input signal as informative as possible, only the excitation parts must be considered. In addition, to average out mild nonlinearities from the identification process, excitation sequences of different amplitudes should be employed. To this purpose, for each identification campaign one input signal is obtained by concatenating three distinct excitations with different amplitude in ascending order, as depicted in Figure 3a. As discussed in [15], the concatenation of data segments can cause artificial transients that may degrade the quality of the estimate. While this is in principle an important issue, in the present work it represents a negligible effect due to the small number of concatenations and the large duration of the considered sequences. For the sake of conciseness, in this paper only the results obtained using as input a signal resulting from the concatenation of three PRBS excitation sequences belonging to the fourth identification campaign are presented. A graphical representation of this signal in time and frequency domain is showed in Figure 3. As can be seen, the cutoff frequency of the input signal complies with the quadrotor dominant attitude dynamics.

Finally, during the tests the following variables were logged, with sampling time equal to 0.02 s: input control variable u, pitch angular acceleration $\dot{q}$, angular

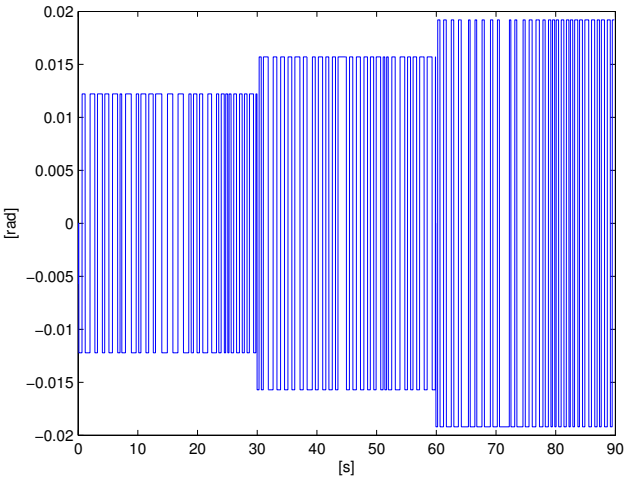

(a) *Time domain.*

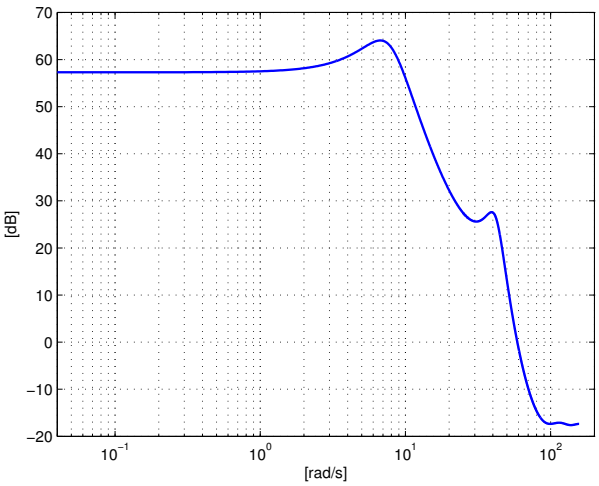

(b) *Frequency domain.*

Figure 3: Input PRBS signal for system identification.

velocity q and angle θ measured by the on-board Inertial Measurement Unit (IMU).

3. BLACK-BOX MODEL IDENTIFICATION

The problem of black-box model identification for the attitude dynamics of hovering quadrotors has been studied extensively in the literature (see, *e.g.*, [2, 4, 6] and the references therein for a detailed discussion). In particular, from the cited references, subspace model identification (SMI) methods emerge as a viable approach for the task. In view of this, the identification algorithm selected for this work belongs to the MOESP (Multivariable Output Error State Space model realization) class of subspace identification methods and is known in the literature as PI-MOESP (see, *e.g.*, [20]). This algorithm, which is briefly described in the following, considers the finite dimensional, linear time-

invariant (LTI) state space model class

(1)
$$\begin{aligned} x_{t+1} &= Ax_t + Bu_t \\ \tilde{y}_t &= Cx_t + Du_t \end{aligned} \qquad y_t = \tilde{y}_t + v_t$$

where $x_t \in \mathbb{R}^n$, $u_t \in \mathbb{R}^m$, $y_t \in \mathbb{R}^p$ and v_t is an additive perturbations to be defined in more detail in the following. The algorithm proceeds in three steps. The first problem is the consistent estimation of the column space of the extended observability matrix Γ, defined as:

$$\Gamma = \begin{bmatrix} C \\ CA \\ \vdots \\ CA^{i-1} \end{bmatrix}$$

from measured input-output samples $\{u_t, y_t\}$. On the basis of such an estimate, the A and C matrices of the model can be determined, by exploiting the shift-invariance of the observability subspace. Finally, a linear least squares problem is solved in order to determine the B and D matrices[1]. One important equation in the derivation of SMI algorithms is a data equation relating (block) Hankel matrices constructed from the i-o data samples. Let the following block-Hankel matrices be defined:

$$Y_{t,i,j} = \begin{bmatrix} y_t & y_{t+1} & \cdots & y_{t+j-1} \\ y_{t+1} & y_{t+2} & \cdots & y_{t+j} \\ \vdots & \vdots & \ddots & \vdots \\ y_{t+i-1} & y_{t+i} & \cdots & y_{t+i+j-2} \end{bmatrix}$$

$$U_{t,i,j} = \begin{bmatrix} u_t & u_{t+1} & \cdots & u_{t+j-1} \\ u_{t+1} & u_{t+2} & \cdots & u_{t+j} \\ \vdots & \vdots & \ddots & \vdots \\ u_{t+i-1} & u_{t+i} & \cdots & u_{t+i+j-2} \end{bmatrix}$$

$$X_{t,j} = \begin{bmatrix} x_t & x_{t+1} & \cdots & x_{t+j-1} \end{bmatrix}$$

and let the following block-Toeplitz matrix be defined:

$$H = \begin{bmatrix} D & 0 & \cdots & 0 \\ CB & D & \cdots & 0 \\ CAB & CB & \cdots & 0 \\ \vdots & \vdots & \vdots & \vdots \\ CA^{i-2}B & CA^{i-3}B & \cdots & D \end{bmatrix}. \tag{2}$$

Considering the special case of absence of noise terms, the data equation is compactly denoted as:

$$Y_{t,i,j} = \Gamma X_{t,j} + HU_{t,i,j}. \tag{3}$$

On the basis of the data equation, the PI-MOESP algorithm considers the RQ factorization:

$$\begin{bmatrix} U_{t+i,i,j} \\ U_{t,i,j} \\ Y_{t+i,i,j} \end{bmatrix} = \begin{bmatrix} R_{11} & 0 & 0 \\ R_{21} & R_{22} & 0 \\ R_{31} & R_{32} & R_{33} \end{bmatrix} \begin{bmatrix} Q_1 \\ Q_2 \\ Q_3 \end{bmatrix}. \tag{4}$$

[1]Indeed, the forced response of the output y is a linear function of the elements of B and D.

Then, a consistent estimate of the column space of Γ is provided via a SVD of the matrix R_{32} under the assumption that v_t is an ergodic sequence of finite variance, satisfying $E[u_t v_s^T] = 0 \ \forall t, s$.

The presence of a time delay in the plant dynamics appears in the model identified via the PI-MOESP algorithms as a non-minimum phase zero. To account for the time delay in a proper way, a forward shift of a proper number of samples on data sets input signal u was applied before identification. In order to reintroduce the delay removed from the model into the control scheme, a correspondent time shift was added in simulation. The overall delay of the control loop implemented on board (from IMU measurements, through acquisition and processing, to servo actuation of blade collective pitch) was estimated in the range between 0.05 s and 0.1 s: adopted shift is equal to three samples, corresponding to $\hat{\tau} = 0.06$ s.

For the sake of comparison, another black-box model identification method is taken into account in this work. In particular, an on-line implementation of the classical Least Mean Squares (LMS) algorithm is considered, which updates recursively on-board an estimate of the SISO discrete-time impulse response of pitch angular velocity q in the form of the Finite Impulse Response (FIR) model

$$y_t = w_1 u_{t-1} + w_2 u_{t-2} + \ldots + w_r u_{t-r}, \tag{5}$$

see [15]. A state space model for the pitch dynamics can then be recovered from the estimated impulse response $w_i, \quad i = 1, \ldots, r$ via suitable realization techniques (specifically, Kung's algorithm, see, again, [15], has been employed).

4. GREY-BOX MODEL IDENTIFICATION

Unlike the black-box models discussed in the previous section, which are parameterised in an unstructured way, grey-box models have a physically motivated structured parameterisation, derived from first principle considerations. In this case, in order to work out such a parameterisation, the equations governing the quadrotor pitch dynamics must be introduced.

4.1 Model structure

The dynamic model described in this section adds aerodynamic terms to the basic quadrotor rigid body dynamics model. Let $\mathcal{I}$ be the right-hand inertial frame and $\mathcal{B}$ the right-hand body-fixed frame. The orientation of the rigid body is given by a rotation matrix $R : \mathcal{B} \to \mathcal{I}$ and the Euler angles that describes this rotation at time t are

$$\Phi(t) = \big(\varphi(t), \theta(t), \psi(t)\big).$$

Let I denote the constant inertia matrix expressed in the body fixed frame, assumed to be diagonal for the

sake of simplicity

$$I = \begin{bmatrix} I_{xx} & 0 & 0 \\ 0 & I_{yy} & 0 \\ 0 & 0 & I_{zz} \end{bmatrix}.$$

Denoting $\omega(t) = \big(p(t), q(t), r(t)\big)$ the angular velocity expressed in the body-fixed frame at time t, the differential equation governing the evolution of the pitch angular velocity is

$$\begin{aligned} I_{yy}\,\dot{q}(t) = (I_{zz} - I_{xx})\,p(t)\,r(t) + \frac{\partial M}{\partial q}\,q(t) + \\ + \frac{\partial M}{\partial u}\,u(t-\hat{\tau}) \end{aligned} \tag{6}$$

where $\frac{\partial M}{\partial q}$ is the stability derivative of the vehicle pitch moment with respect to q (see [17]), *i.e.*,

$$\frac{\partial M}{\partial q} = -2\rho A \left(\bar{\Omega} R\right)^2 \frac{\partial C_T}{\partial q} d$$

and $\frac{\partial C_T}{\partial q}$ is the variation of the thrust coefficient with respect to q, given by

$$\frac{\partial C_T}{\partial q} = \frac{C_{l_\alpha}}{8}\frac{\sigma}{\bar{\Omega} R} d.$$

In (6) the control derivative of the pitch moment with respect to the input (see [18]) is expressed as

$$\frac{\partial M}{\partial u} = \rho A_b \left(\bar{\Omega} R\right)^2 \frac{\partial \frac{C_T}{\sigma}}{\partial \theta_R} d.$$

The evolution of the Euler angles is related to the angular velocity through the following equation

$$\dot{\boldsymbol{R}}(t) = \boldsymbol{R}(t) \cdot \mathrm{sk}\big(\omega(t)\big), \tag{7}$$

where $\mathrm{sk}(\cdot)$ is the skew-symmetric matrix such that $\mathrm{sk}(a)\,b = a \times b$ for vectors in $\mathbb{R}^3$. Expanding (7), the evolution of the pitch attitude is

$$\dot{\theta}(t) = \cos\big(\varphi(t)\big) q(t) - sin\big(\varphi(t)\big) r(t). \tag{8}$$

Since on the test bed the roll and yaw rotational and all translational DoFs are constrained, from (6) and (8) it follows that

$$\begin{aligned} I_{yy}\dot{q}(t) &= \frac{\partial M}{\partial q}\,q(t) + \frac{\partial M}{\partial u}\,u(t-\hat{\tau}) \\ \dot{\theta}(t) &= q(t). \end{aligned}$$

The IMU is not rigidly connected to quadrotor airframe: in order to have reliable measurements, a vibration damping system must be included in the model as a simple rotational mass-spring-damper

$$\begin{aligned} I_{yy}\dot{q}(t) &= \frac{\partial M}{\partial q}\,q(t) + \frac{\partial M}{\partial u}\,u(t-\hat{\tau}) + \\ &\quad + k\big(\theta_P(t) - \theta(t)\big) + c\big(q_P(t) - q(t)\big) \\ J\dot{q}_P(t) &= -k\big(\theta_P(t) - \theta(t)\big) - c\big(q_P(t) - q(t)\big) \\ \dot{\theta}(t) &= q(t) \\ \dot{\theta}_P(t) &= q_P(t) \end{aligned} \tag{9}$$

where q_P and θ_P represent the vehicle angular pitch velocity and the pitch angle measured by the IMU respectively. System (9) can be rewritten in state space form as

$$\begin{aligned} \dot{x}(t) &= Ax(t) + Bu(t-\hat{\tau}) \\ y(t) &= Cx(t) + Du(t-\hat{\tau}) + v(t) \end{aligned} \tag{10}$$

where $x(t) = \big(q(t), q_P(t), \theta(t), \theta_P(t)\big)$ is the state vector and

$$A = \begin{bmatrix} \frac{1}{I_{yy}}\frac{\partial M}{\partial q} - \frac{c}{I_{yy}} & \frac{c}{I_{yy}} & -\frac{k}{I_{yy}} & \frac{k}{I_{yy}} \\ \frac{c}{J} & -\frac{c}{J} & \frac{k}{J} & -\frac{k}{J} \\ 1 & 0 & 0 & 0 \\ 0 & 1 & 0 & 0 \end{bmatrix}$$

$$B = \begin{bmatrix} \frac{1}{I_{yy}}\frac{\partial M}{\partial u} \\ 0 \\ 0 \\ 0 \end{bmatrix}$$

$$C = \begin{bmatrix} 0 & 1 & 0 & 0 \end{bmatrix}, \quad D = \begin{bmatrix} 0 \end{bmatrix}.$$

In (10) v represents the measurement noise, introduced as a Gaussian process with zero mean and variance Q.

4.2 Parameter estimation

In this section the approaches considered for the estimation of the parametric model class derived in the previous one are presented and discussed. In particular, the quadrotor inertia was measured through a specific identification procedure (see [7]) and was found to be $I_{xx} = I_{yy} = 0.1705\,\mathrm{kg\,m^2}$ and $I_{zz} = 0.3206\,\mathrm{kg\,m^2}$. Thus, the unknown parameters in system (10) are:

$$\Theta = \left(\frac{\partial M}{\partial q}, \frac{\partial M}{\partial u}, k, c, J\right).$$

4.2.1 Maximum likelihood estimation

The most common estimator for an output-error model, such (10), is the maximum likelihood (ML) estimator. Suppose that a dataset $\{u(t_i), y(t_i)\}$, $i \in [1, N]$ of sampled input/output data from system (10) is available. The ML estimate is equal to the value of Θ that maximizes the likelihood function, which is the probability density function of y given Θ, *i.e.*,

$$\mathbb{L}(y, \Theta) = \mathrm{P}(y \mid \Theta)$$

If $\mathrm{P}(y)$ is Gaussian, as in (10), the ML estimator minimizes a positive function of the prediction error (see [13] for details about the implementation of the maximum likelihood scheme for output-error state space models).

4.2.2 Time-frequency domain estimation

The downside of the black-box model identification approaches, such as the ones proposed in Section 3, is

the impossibility to enforce *a-priori* information on the model structure. This information is easily imposed in a grey-box model approach, however the batch nature of SMI methods make them more attractive with respect to output-error ones, which typically have an iterative nature. One might consider the idea of using the black-box model obtained via SMI to initialize the output-error iteration; while the idea is attractive, it suffers from a major weakness, namely the fact that state space models obtained from SMI methods are expressed in a state space basis which cannot be given any physical interpretation. A novel technique for bridge the gap between unstructured models and structured ones was proposed in [4]. This procedure takes advantage of frequency domain approaches, using an $\mathscr{H}_\infty$ model matching method to relate unstructured models computed using SMI techniques to structured ones determined from first principles. As it will be explained further, in this approach the subspace model and the grey-box model will be compared. However, the first one is a discrete-time model whereas the grey-box is a continuous-time model. Conversion of the discrete LTI subspace model to continuous-time is the fist step of this method. In this work, this conversion assumes a zero order hold on the inputs.

Let $\mathcal{M}_{ns}$ be the LTI unstructured black-box model identified using the PI-MOESP algorithm in Section 3 and $\mathcal{M}_s(\Theta)$ be the structured model described in (10). Since the two models describe the same real system with different state space basis, they should have the same input-output behavior. This behavior, for linear time-invariant systems, can be represented in terms of the transfer function. Let $G_{ns}(s)$ and $G_s(s,\Theta)$ denote the transfer function of $\mathcal{M}_{ns}$ and $\mathcal{M}_s(\Theta)$ respectively. The model matching problem can be effectively resolved seeking the value of Θ that minimizes a suitably chosen norm of the difference between the two transfer functions. The infinity norm is considered, thus the problem can be recast as

$$\hat{\Theta} = \arg\min_{\Theta} \|G_{ns}(s) - G_s(s,\Theta)\|_\infty \tag{11}$$

where the infinity norm of an asymptotically stable linear time-invariant system with transfer function $G(s)$ is defined as

$$\begin{aligned}\|G\|_\infty &= \sup_{\alpha>0}\left\{\sup_{\omega}\bar{\sigma}\Big(G(\alpha+j\omega)\Big)\right\}\\ &= \sup_{\omega}\bar{\sigma}\Big(G(j\omega)\Big)\end{aligned}$$

where $\bar{\sigma}$ is the maximum singular value.

Since $\mathcal{M}_s(\Theta)$ has to match $\mathcal{M}_{ns}$ in the frequency range where $\mathcal{M}_{ns}$ well describes the real system, a suitable filter G_W has to be introduced to focus the matching on this range, as showed in Figure 4.
The problem (11) is therefore rewritten as

$$\hat{\Theta} = \arg\min_{\Theta} \big\|G_W(s)\big(G_{ns}(s) - G_s(s,\Theta)\big)\big\|_\infty .$$

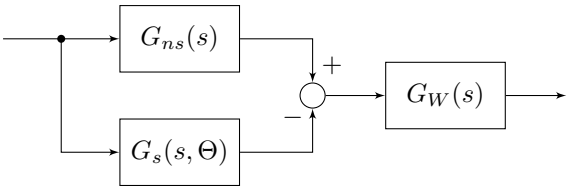

Figure 4: Block diagram of time-frequency domain approach with filter.

Algorithm	VAF with first validation dataset	VAF with second validation dataset
LMS	23.3 %	71.5 %
PI-MOESP	64.4 %	71 %
ML	58.4 %	64.9 %
$\mathscr{H}_\infty$	60.1 %	64.1 %

Table 2: Variance Accounted For (VAF) corresponding to each algorithm.

This non-convex, non-smooth optimization problem can be solved by exploiting reliable computational tools developed for the solution of the (mathematically equivalent) problem of fixed-structure robust controller design (see [8]).

In the above discussion, the assumption that $\mathcal{M}_{ns}$ and $\mathcal{M}_s(\Theta)$ describe the same real system was made. Since the closed-loop time delay was removed in the subspace model identification method with a forward shift of the input signal u, the same delay has to be removed from $\mathcal{M}_s(\Theta)$ setting $\tau = 0$. Later, the delay can be easily reintroduced by setting τ to the estimated value.

5. RESULTS AND VALIDATION

In this section the results obtained in the identification of linear models for the Aermatica ANTEOS UAV are presented and discussed. In particular, in Sections 5.1 and 5.2 the procedures used to obtain black-box and grey-box models from data are illustrated, while Section 5.3 is devoted to the discussion of the results.

5.1 Black-box models

The PI-MOESP algorithm described in Section 3 has been applied to identify SISO models having as input the control variable corresponding to the difference between the pitch angles applied to the front and back rotors (the time history of which is the combination of the excitation of the PRBS and the feedback action provided by the on-board controller executing the supervision task) and as output the angular rate of the pitch axis of the quadrotor.

The model order and the hyperparameter i corresponding to the number of rows in the Hankel matrices constructed from data have been chosen by means of

a cross-validation approach, namely: the identification has been carried out for various values, in a predefined range, for model order n and block-size parameter i of the data matrices; the performance of each obtained model has been assessed on the validation portion of the data set, in terms of the Variance Accounted For (VAF) indicator for the simulated response of the identified models. Then, the combination of model order and block-size that maximizes the VAF of the cross validation dataset has been retained. In particular, the predefined range of model order is from 1 to 5 while the the range of the block-size data matrices is from 10 to 50. The best result of the identification process is obtained with $n = 4$ and $p = 40$.

5.2 Grey-box models

Similarly, the approaches to grey-box modeling outlined in Section 4 have been applied to the problem of modeling the pitch rate response of the quadrotor. In particular, while the maximum likelihood approach does not offer specific parameters to be tuned, in time frequency domain approach the filter G_W is a parameter of the algorithm that has to be tuned to reach the best performance in terms of VAF using a cross validation dataset.

Since the subspace model provides an accurate description of the real system only in the frequency range where the system is excited, G_W is a low-pass filter with an order between 1 and 25 and a cutoff frequency between 3 rad/s and 60 rad/s. The results in Table 2 are achieved using a 15th order low-pass Butterworth filter with a cutoff frequency of 7 rad/s. The cutoff frequency of the filter complies with the excitation frequency of identification input signal.

5.3 Validation and discussion

As outlined in Section 2, the identified models have been validated using two new datasets. The former dataset corresponds to normal closed-loop operation of the pitch control system. Since it represents a typical flight condition, the validation on this dataset provides an assessment of the real performance of the models. This dataset is obtained by imposing a desired angular reference manually and measuring the closed-loop response when the nominal attitude controller is enabled (Figure 5). As illustrated in Section 2, this process is done at the end of each identification test. Since it does not depend on the parameters of the PRBS sequence in the test, the validation dataset is selected randomly between all the identification tests.

The latter validation dataset, on the other hand, is a single PRBS excitation signal with an amplitude of 0.015 rad and a switching interval between 0.4 s and 0.8 s that was not employed in the identification process. This dataset allows to assess the performance of the identification campaign therefore the values of the identification algorithm parameters are chosen to maximize the matching between the model output and this dataset in terms of VAF.

In Figure 6 the measured pitch rate and the simulated ones obtained from the identified models are compared using the first validation dataset as input, while the Figure 7 shows the same results exploiting the second validation dataset. The VAF corresponding to each model is reported in Table 2 for both the validation datasets.

As far as black-box models are concerned, it can be seen from the figures and the table that the model obtained using the LMS algorithm provides good performance using the excitation validation signal, but its ability to replicate the data degrades significantly when it is applied to data corresponding to normal closed-loop operation. The LMS algorithm is deeply tied with the identification signal and therefore it leads to the least accurate model since it has poor generalization capability. On the contrary, the PI-MOESP subspace method leads to a black-box model with the best validation performance, on both the considered datasets.

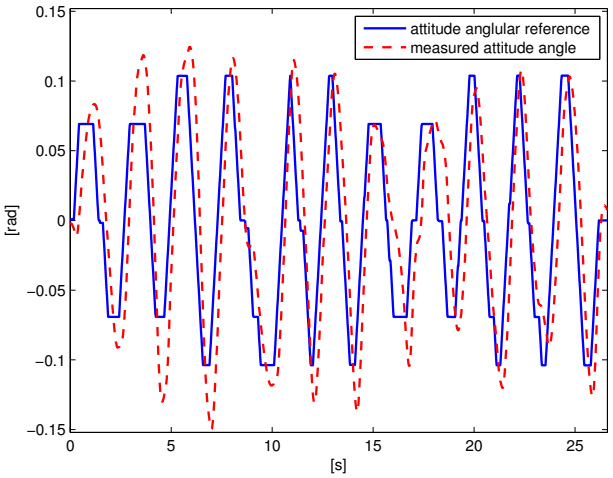

Figure 5: The attitude angular reference and the measured attitude angle of the first validation dataset.

As for the grey-box models, it is well known in the literature (see, for example, the classical paper [11]) that as they have a fixed structure to deal with a-priori information, normally they lead to inferior performance with respect to black-box models. Indeed, as reported in Table 2, this is the case also for the application under study, as the two grey-box models perform sightly less satisfactorily than the SMI black-box one. It is interesting to point out that similar conclusions have been reached in a related study (see [5]) devoted to the identification of the flight dynamics of a full scale helicopter. Finally, since, as explained in Section 4, the time-frequency domain approach deals with a model matching problem, it is also interesting

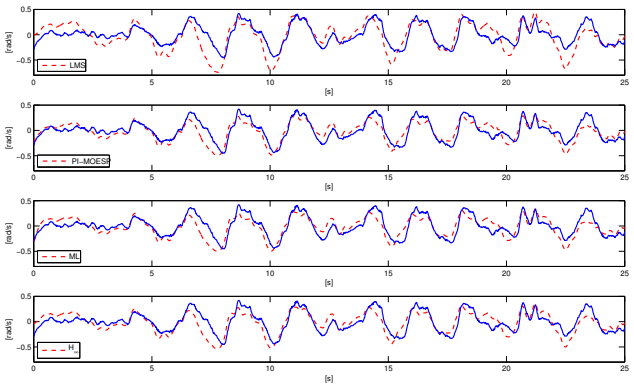

Figure 6: Validation of the identified models with the normal closed-loop operation dataset (blue lines: measured pitch rate; red dashed lines: model simulations).

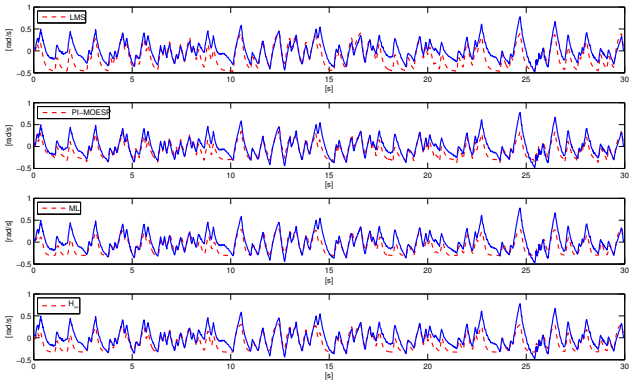

Figure 7: Validation of the identified models with the excitation dataset (blue lines: measured pitch rate; red dashed lines: model simulations).

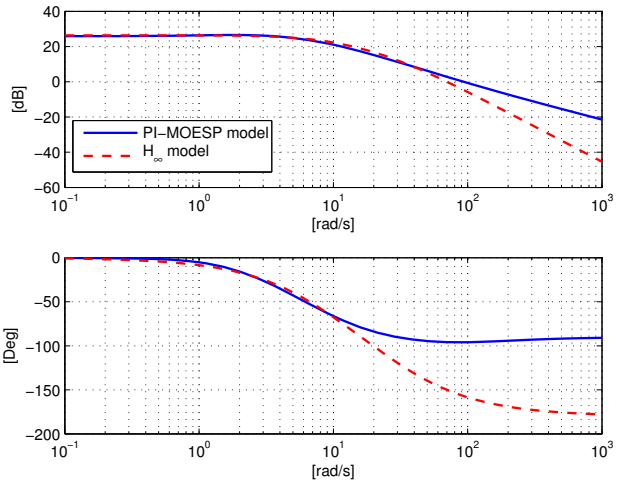

Figure 8: Bode diagrams of the PI-MOESP model and the $\mathscr{H}_\infty$ model.

to compare the frequency response of the black-box SMI model to the frequency response of the grey-box one obtained from the time-frequency domain method. As showed in Figure 8, where the Bode diagrams of the PI-MOESP model and the model identified with the $\mathscr{H}_\infty$ algorithm are illustrated, the match between the two models is quite accurate before the cutoff frequency of the filter with VAF = 96.9% using the excitation validation dataset as input.

6. CONCLUSIONS

The problem of characterizing the attitude dynamics of a variable pitch quadrotor has been considered and a number of approaches to its identification have been applied to data collected on the real quadrotor, in laboratory conditions. In view of both its non-iterative nature and the accurate performance in replicating the experimental data, the subspace approach appears to be a good candidate for the identification part of a fast, highly automated control design tool chain for quadrotor attitude.

REFERENCES

[1] P. Apkarian, D. Noll. Nonsmooth H_∞ synthesis. *IEEE Transactions on Automatic Control*, 51(1):229-244, 2006.

[2] M. Bergamasco, M. Lovera. Continuous-time predictor-based subspace identification for helicopter dynamics. In *37th European Rotorcraft Forum*, Gallarate, Italy, 2011.

[3] M. Bergamasco, M. Lovera. State space model identification: from unstructured to structured models with an H_∞ approach. In *5th IFAC Symposium on System Structure and Control*, Grenoble, France, 2013.

[4] M. Bergamasco, M. Lovera. Rotorcraft system identification: an integrated time-frequency domain approach. *Advances in Aerospace Guidance, Navigation and Control*, Springer:161-181, 2013.

[5] M. Bergamasco, A. Ragazzi, M. Lovera. Rotorcraft system identification: a time/frequency domain approach. In *IFAC World Congress*, Cape Town, South Africa, 2014.

[6] M. Bergamasco, M. Lovera. Identification of linear models for the dynamics of a hovering quadrotor. *IEEE Transactions on Control Systems Technology*, available on-line, 2014.

[7] C.L. Bottasso, D. Leonello, A. Maffezzoli, F. Riccardi. A procedure for the identification of the inertial properties of small-size RUAVs. *35th European Rotorcraft Forum*, 2009.

[8] P. Gahinet, P. Apkarian. Decentralized and fixed-structure H_∞ control in MATLAB. *50th IEEE Conference on Decision and Control and European Control Conference*, Orlando, USA, 2011.

[9] P. Hamel, J. Kaletka. Advances in rotorcraft system identification. *Progress in Aerospace Sciences*, 33(3-4):259-284,1997.

[10] R. Jategaonkar. *Flight Vehicle System Identification.* AIAA, 2006.

[11] C.G. Källstrom, K.J. Åstrom. Experiences of system identification applied to ship steering. *Automatica*,17(1):187-198, 1981.

[12] S. K. Kim, D. Tilbury. Mathematical modeling and experimental identification of an unmanned helicopter robot with flybar dynamics. *Journal of Robotic Systems*, 21(3):95-116, 2004.

[13] V. Klein, E.A. Morelli. *Aircraft system identification: theory and practice.* AIAA, 2006.

[14] M. La Civita, W. Messner, T. Kanade. Modelling of small-scale helicopters with integrated first-principles ans system identification techniques. In *Proceedings of the 58th American Helicopter Society Annual Forum*, 2002.

[15] L. Ljung. *System identification: theory for the user*, 2nd ed. PTR Prentice Hall, 1999.

[16] R. Mahony, V. Kumar. Aerial robotics and the quadrotor [from the guest editors]. *IEEE Robotics Automation Magazine*, 19(3):19-19, 2012.

[17] P. Pounds, R. Mahony, P. Corke. Modelling and control of a large quadrotor robot. *Control Engineering Practice*, 18(7):691-699 2010

[18] R.W. Prouty. *Helicopter Performance, Stability, and Control.* Krieger Publishing Company, 1990.

[19] M. Tischler, R. Remple. *Aircraft And Rotorcraft System Identification: Engineering Methods With Flightest Examples.* AIAA, 2006.

[20] M. Verhaegen, V. Verdult. *Filtering and System Identification: A Least Squares Approach.* Cambridge University Press, 2007.